

Original Research Articles

Assessing Shoreline Changes in Pagatan Beach, South Kalimantan, Indonesia: A Remote Sensing Approach using Satellite Imagery

Ahmad Azmi Fitriadina*, Dyah Pradhitya Hardiania, Elia Anggarinia

^a Department of Civil Engineering, Universitas Muhammadiyah Banjarmasin, Banjarmasin, Indonesia

*Corresponding author: azmi.fitr@gmail.com

Highlights:

- Conducting a case study to assess shoreline changes over 30+ years using publicly available satellite imagery and the CoastSat toolkit at Pagatan Beach.
- Estimating erosion and accretion rates over the study period and mapping coastal changes, including future projections in Pagatan Beach.
- Addressing challenges in satellite-derived shorelines such as variation in image quality over time and frequent cloud cover.

Abstract: Pagatan Beach, located in South Kalimantan, Indonesia, has experienced substantial shoreline changes over the past few decades, posing potential risks to local ecosystems, infrastructure, and communities. This study examines the shoreline dynamics of Pagatan Beach from 1990 to 2023 using satellite imagery data from Landsat 5, Landsat 7, and Landsat 8. Utilizing the CoastSat toolkit, known for its georeferencing accuracy within 10 meters, shoreline positions were extracted from a total of 492 satellite images. The analysis identifies distinct patterns of erosion and accretion across different transects, influenced by natural forces such as wave action, currents, tides, and wind, as well as human interventions, particularly the construction of jetties and groins. The study highlights the critical role of satellite technology in monitoring coastal changes, providing valuable insights where in situ measurements are unavailable. Projection of shoreline changes suggest continued accretion in areas near installed groins, as the groins effectively retain sediment within their maximum length. Similarly, sections around the jetty at the easternmost part show a stable accretion trend, indicating effective sediment control. In contrast, a persistent erosion trend is anticipated along a 1-kilometer stretch in the central zone, potentially reducing the beach area by 2025. Without intervention, there is a risk of erosion encroaching onto adjacent roads by 2028. Despite challenges such as varying image quality and cloud cover, the findings underscore the importance of satellite-based monitoring for effective coastal management and planning.

Keywords: erosion; satellite imagery; shoreline changes

1. Introduction

Coastlines represent dynamic interfaces between land and sea, influenced by factors, such as sediment movement, erosion, storms, sea levels, waves, currents and human activities. The changes in coastline boundaries possess significant importance for coastal management, development planning, and environmental protection [1, 2]. In order to define the boundary, Boak and Turner [3] classify shoreline extraction into three categories: (i) using visual shoreline indicators, (ii) referencing specific tidal data, and (iii) employing image-processing methods. Long-term variation in coastline positions serve as crucial indicators of regional depositional or erosional process, requiring analyzing grounded in historical records [4].

Coastal erosion and changes in its variability are major challenges that require close monitoring and management [5]. Effective coastal management is critical not only for mitigating erosion, but also for managing natural resources and protecting habitat. To maintain the sustainability and resilience of infrastructure, such as residential areas, highways, and bridges, near the coastal environment, strategic planning needs to consider the changing position of shorelines. Therefore, risk assessment for coastal infrastructure has been critical for mitigating the possible effects of shoreline retreat and maintaining long-term stability and safety.

In recent years, there has been a significant focus on developing methodologies to effectively monitor and analyze shoreline changes using satellite imagery. The advent of Google Earth Engine [6] has been instrumental in this effort, providing low-cost satellite images accessible worldwide for the past three decades to detect coastal change [7-9]. Satellite images can cover a large area, enabling faster acquisition and processing of data. These images provide a certain level of detail, with multispectral bands helping to clearly define the water and boundary interface [8]. The ability to

Received: 14 June 2024 Revised: 18 June 2024 Accepted: 20 June 2024 Published: 22 June 2024



monitor changes in coastal morphology at various temporal and spatial scales using satellite-derived data can significantly reduce the amount of in situ measurements needed, thereby lowering the cost of monitoring activities [7].

Global-scale studies have demonstrated the effectiveness of satellite imagery in assessing erosion and accretion trends across the world's beaches [10, 11]. For example, both Luijendijk, et al. [10] and Vousdoukas, et al. [11] utilized the Google Earth Engine (GEE) platform to conduct long-term observations of average annual shoreline changes. These assessments provide a comprehensive picture of coastal changes and help identify critical erosion areas on the world's beaches. However, they may not fully account for the influence of local processes on coastal dynamics, which is essential for precise estimates of coastal change. In local-scale studies, the application of satellite data focuses primarily on mid-term and long-term coastline evolution [7, 8, 12, 13-15]. These studies commonly suggest that the image composite technique can effectively identify shoreline changes, with accuracy expected to improve as image pixel resolution increases.

One of the state-of-the-art tools recently developed is the open-source tool CoastSat [9], which automatically detects waterlines on beaches using publicly available satellite imagery. This tool has been validated for various coasts around the globe, and its accessibility has led to widespread application in estimating coastal changes [7, 8, 13, 15]. CoastSat is recognized for its accuracy of approximately 10 meters, achieved through a sub-pixel resolution technique that enhances the standard 30-meter pixel resolution provided by publicly available satellites. The algorithm in this toolkit enhances the spatial resolution of satellite images, removes cloudy pixels, and employs supervised image classification with sub-pixel border segmentation to accurately map shoreline positions.

This research is a case study focusing on Pagatan Beach, located in South Kalimantan, Indonesia. Over recent decades, Pagatan Beach has experienced significant shoreline changes, posing potential risks to local ecosystems, infrastructure, and communities. It is reported that man-made structures have altered the nature of coastal change, including jetties built downstream of rivers near Pagatan Beach and groins constructed in 2021 to maintain the shoreline retreat. The primary objective of this study is to estimate the long-term and mid-term trends of shoreline change at Pagatan Beach by using CoastSat toolkit. Specifically, the research aims to (i) quantify the rates of shoreline erosion and accretion and (ii) map the risks to nearby infrastructure due to these shoreline changes. By addressing these objectives, the study seeks to contribute to the field by providing detailed insights into the dynamics of shoreline change and their implications for coastal management and infrastructure planning in Pagatan Beach.

2. Methodology

2.1. Study Area

The study area for this research is Pagatan Beach, located in South Kalimantan, Indonesia (see Figure 1). Pagatan is a coastal city situated in the Kusan Hilir District of Tanah Bumbu Regency in South Kalimantan. The observation area spans 1.7 kilometers, positioned around 1.5 kilometers from the central city of Pagatan.

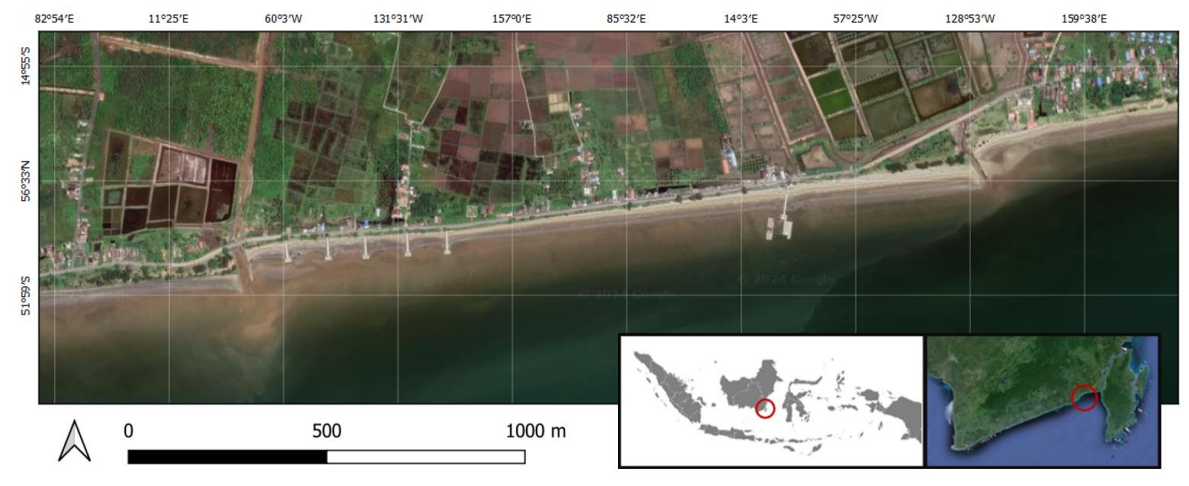


Figure 1. Google Earth Image of Pagatan Beach, South Kalimantan, Taken in 2023

Pagatan Beach is characterized by its grey/black sandy shores, typical of South Kalimantan's coastline, known for its relatively calm wave conditions predominantly from the south and southeast directions [16]. According to satellite altimetry data evaluated by Alifdini, et al. [17], the tidal range in Pagatan Beach is between 0.3 and 0.4 meters, which is relatively moderate and influences coastal dynamics and sediment transport. Infrastructure around the beach includes a main road that runs along the coast, providing connectivity to the central city, and two main bridges that are crucial for transportation and accessibility.

2.2. Data Collection and Image Retrieval

The shoreline data for Pagatan Beach was obtained using the CoastSat toolkit, which accessed publicly available satellite imagery from the Google Earth Engine (GEE). The required satellite missions were Landsat 5, Landsat 7, and Landsat 8, covering the period from 1990 to 2023. The selection of this period considers the availability and continuity of satellite data across different missions covering Pagatan Beach (see Table 1 for details). The selected spectral bands for shoreline detection were the three visible bands (R, G, B), the near-infrared band (NIR), the short-wave infrared band (SWIR1), and panchromatic band.

| Table 1. Satellite Data Information from GGE for Region of Interest in Pagatan Beach |
|---|
|---|

| Satellite Missions | Number of Images Available | Time Period | Revisit Period | Pixel size (visible bands) |
|-----------------------|-------------------------------|----------------|-------------------|---|
| Landsat 5 | 240 | 1990 – 2011 | 16 days | 30 m R, G, B, NIR, SWIR1 bands |
| Landsat 7 | 692 | 1999 – 2023 | 16 days | 30 m R, G, B, NIR, SWIR1 bands + 15 m panchromatic band |
| Landsat 8 | 384 | 2013 - 2023 | 16 days | 30 m R, G, B, NIR, SWIR1 bands + 15 m panchromatic band |

Potential biases in data selection and image retrieval arise due to varying image quality from different satellite missions. Landsat 5 (1990-2011), Landsat 7 (from 1999, with data gaps since 2003), and Landsat 8 (from 2013) provide images of increasing quality. The rapid improvement in satellite remote sensing means newer data may capture finer details. Data before 2013, especially from Landsat 7, may be less reliable due to resolution and coverage issues stemming from reported satellite mission problems, leading to data gaps in retrieved images. Despite these challenges, usable data can still be extracted for regions of interest, such as Pagatan Beach, for this study.

2.3.CoastSat Toolkit

The selection of the CoastSat toolkit for this study is well-justified by several key factors. CoastSat is an open-source tool that automatically detects waterlines on sandy beaches using publicly available satellite imagery, which operates under open-data policies. This tool has been validated for various coastlines globally, demonstrating its reliability and robustness in diverse settings. Its accessibility and ease of use have led to widespread application in estimating coastal changes [7, 8, 13, 15]. CoastSat is recognized for its horizontal precision of approximately 10 meters, achieved through a sub-pixel resolution technique that enhances the standard 30-meter spatial resolution of available satellite images. CoastSat toolkit is accessible for free on GitHub. Settings for the shoreline extraction used for this study is provided in Table 2.

2.3.1. Work Labor Image Pre-Processing

After downloading the satellite images for the region of interest (Pagatan Beach) within a specified date range, the images undergo pre-processing using the CoastSat toolkit. As Vos, et al. [9] described, this involves two key steps: (i) cloud masking and (ii) panchromatic image sharpening and down-sampling. As for cloud masking, each image retrieved is supplemented by a Quality Assessment band, provided by the USGS for Landsat satellite missions, which includes a per-pixel cloud mask. This Quality Assessment band allows for the calculation of the percentage of cloud cover based on the number of cloudy pixels within the region of interest. In this study, the cloud threshold is set at a

value of 0.1, meaning that all images with more than 10% cloud cover over the defined region of interest were discarded.

Table 2. Setting Parameters in CoastSat for Pagatan Beach

| Parameters | User-defined Settings | | |
|--|---|--|--|
| Date range | From 01-01-1990 to 01-01-2024 | | |
| Satellite missions | Landsat 5, Landsat 7, Landsat 8 | | |
| General parameters: | | | |
| Cloud threshold on the image | o.1 (value between o and 1) | | |
| Distance clouds (buffer around cloud pixels) | 200 meters | | |
| EPSG | 23837 (DGN95 / Indonesia TM-3 zone | | |
| Shoreline detection parameters: | 50.1 | | |
| Minimum beach area | | | |
| Minimum length of shoreline perimeter | 5,000 m² 500 meters | | |
| Sand color | | | |
| Quality control: | Dark (for grey/black sand beaches) | | |
| Check detection | | | |
| | True (shows each shoreline detection to the user for validation) | | |
| Adjust detection | True (allows user to adjust the position of each shoreline by changing the threshold) | | |

Using the CoastSat toolkit, the next pre-processing step is panchromatic image sharpening and down-sampling, which enhances the spatial resolution of satellite images for optimal shoreline detection. For Landsat 7 and Landsat 8 images, the higher resolution panchromatic band increases the resolution from 30 to 15 meters using principal component analysis. Although Landsat 5 lacks a panchromatic band, its 30-meter bands are down-sampled to 15 meters using bilinear interpolation to improve shoreline detection accuracy. Regarding geometric correction, each satellite image retrieved is already orthorectified, meaning it has been corrected for topographic relief, lens distortion, and camera tilt by the data provider (USGS for Landsat). For this study, images with georeferencing accuracy greater than 10 meters were discarded.

2.3.2. Shoreline Detection

In CoastSat's shoreline detection method, as reported by Vos, et al. [9], the pre-processed images are subjected to image classification and sub-pixel resolution border segmentation. In the image classification step, each pixel of the pre-processed image is labeled into one of four classes: 'sand,' 'water,' 'white-water,' and 'other land features' (e.g., vegetation, buildings, rocky headlands). According to Vos, et al. [9], this automatic image classification achieves an accuracy of 99%. In the sub-pixel resolution border segmentation step, the boundary between 'sand' and 'water' in each labeled image is determined using the Modified Normalized Difference Water Index (MNDWI), developed by Xu [18]. The 'sand'/'water' threshold is computed using Otsu's thresholding algorithm, integrated into CoastSat, to maximize inter-class variance. The MNDWI formula is defined as:

$$MNDWI = \frac{SWIR1 - G}{SWIR1 + G} \tag{1}$$

where SWIR1 represents the pixel intensity in the short-wave infrared band and G represents the pixel intensity in the green band. One of the output of shoreline detection steps is a geojson file that can be imported into a GIS application for further analysis.

CoastSat facilitates user supervision for each shoreline extracted from processed images, allowing for visual validation of delineated shorelines. Users can adjust the shoreline positions by modifying the threshold and visually inspecting the MNDWI pixel intensity histogram, ensuring accurate and reliable shoreline detection.

2.4. Estimating Shoreline Trends

Shoreline trends were estimated using the mean cross-shore positions of the extracted shorelines. The cross-shore position represents the horizontal changes in the shoreline over the observed period. Due to the dependence on satellite orbit time and revisit periods, the images are not collected at daily intervals. Instead, only images with less than 10% cloud cover and georeferencing accuracy within 10 meters were selected, resulting in a non-uniform temporal distribution. To estimate the change rate over the years, a linear regression analysis was performed on the selected shoreline positions. The slope of the regression line, indicating the rate of shoreline position changes, was then converted to an annual rate, providing the rate of erosion or accretion in meters per year.

Various statistical measures are utilized to evaluate the variability of shoreline changes derived from satellite imagery analysis. Mean, standard deviation, and Mean Absolute Deviation (MAD) were computed based on the extracted shoreline positions. The mean shoreline position serves as a measure of central tendency, representing the average spatial configuration throughout the study period. Standard deviation quantifies the dispersion or variability of shoreline positions around this mean, offering insights into the extent of shoreline dynamics. Mean Absolute Deviation (MAD) complements these measures by assessing the average magnitude of deviations from the mean shoreline position, providing further insights into the consistency and magnitude of shoreline fluctuations.

2.5. Mapping Risk of Shoreline Changes in Pagatan Beach

The results from CoastSat are provided in GIS to be mapped. Transects, which map the changes in the horizontal position of shorelines over time, are extracted. According to the trends observed in these transects, the risks to nearby roads, infrastructure, and communities are mapped to identify areas vulnerable to erosion and accretion. This process allows for a detailed spatial analysis of the potential impacts on critical infrastructure and settlements due to shoreline changes.

3. Results

3.1. Image Quality Control and Shoreline Extraction

Despite Pagatan Beach's narrow width, shoreline positions were effectively extracted using satellite imagery. Accurate georeferencing is crucial when estimating coastal changes from time series images to ensure observed changes are not due to sensor differences [7]. In this study, satellite images from Landsat missions were used, which were orthorectified and included a Quality Assessment band for cloud pixel identification by the provider (USGS). Only images with less than 10% cloud cover and georeferencing accuracy within 10 meters were selected. After quality control, the analysis included 100 images from Landsat 5, 266 images from Landsat 7, and 126 images from Landsat 8. Each image then underwent user supervision for visual validation of delineated shorelines in CoastSat.

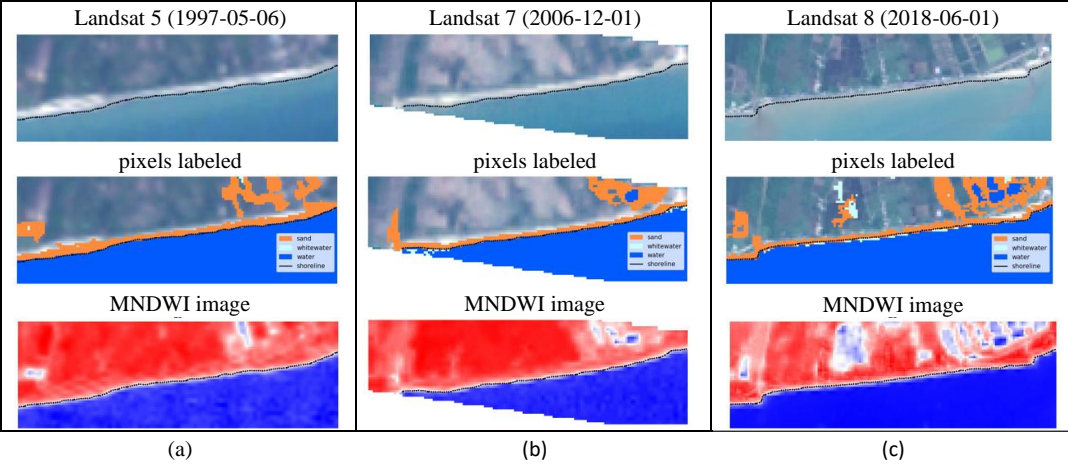


Figure 2. Examples of Coastline Detection using the CoastSat Toolkit (a) Landsat 5; (b) Landsat 7; and (c) Landsat 8. Each Panel Displays the Defined Polygon in the Region of Interest (Top Panel), Labeled Pixels (Middle Panel), and the MNDWI Index Image (Bottom Panel) for Each Satellite Mission. The Extracted Shoreline is Depicted by a Black Line in Each Image.

In this study, Figure 2 presents examples of shoreline extraction using CoastSat from various satellite missions. The figures visually compare resolution quality among the satellite missions, demonstrating CoastSat's capability to extract shoreline positions with varying levels of image clarity and detail.

3.2. Shoreline Changes in Pagatan Beach

The CoastSat toolkit effectively detected and extracted shoreline positions at Pagatan Beach from 1990 to 2023 using satellite imagery. The analysis revealed areas experiencing both accretion and erosion along the shoreline. The extracted shorelines for each year were mapped using GIS as shown in Figure 3, highlighting changes approximately every 6 years from 1996, 2002, 2008, 2014, and 2020, excluding 2023 which shows the latest shoreline position extracted.

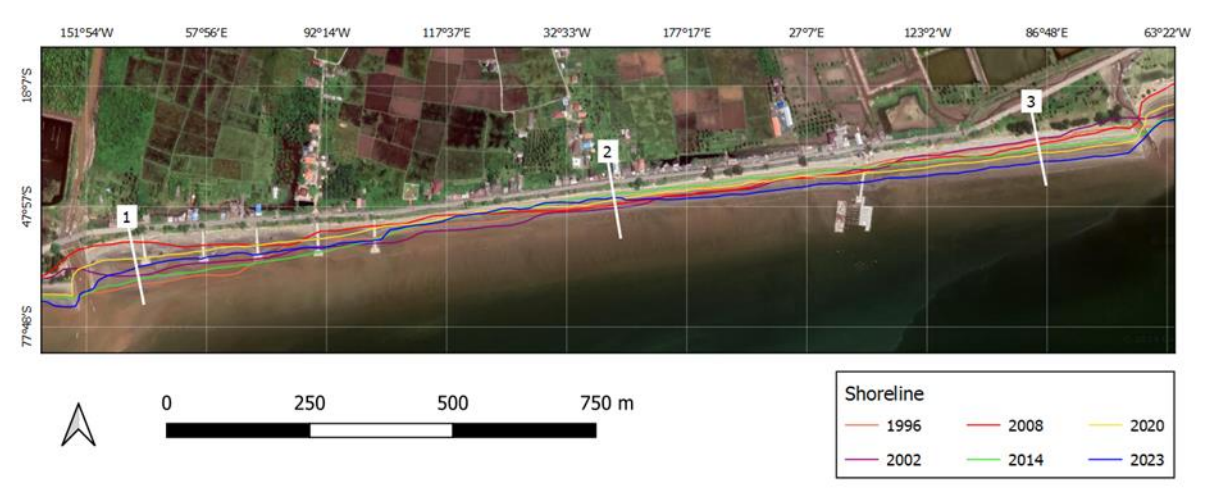


Figure 3. Mapped Shorelines in Pagatan Beach, South Kalimantan

Shoreline change trends were assessed through analysis of three transects (shown in Figure 3). Two transects (Transects 1 and 3) located near the downstream of rivers, adjacent to the study area's periphery where jetties were constructed in the last decade, and one transect (Transect 2) positioned in the narrowest section near the main road at the study area's center. As shown, Transect 1 showed significant variability in shoreline position over the study period, with substantial retreat from 1996 to 2008, recovery in 2014, erosion in 2020, and stability in 2023. Transect 2 exhibited the least variability, but experienced an erosion trend in recent years. Transect 3 tended to experience stable accretion.

The horizontal position of shoreline changes was plotted based on mean shoreline positions observed over a 33-year period, depicted in Figure 4. Variability in shoreline changes was assessed using mean, standard deviation, and mean absolute deviation (MAD). High standard deviation suggest that shoreline positions vary significantly around the mean, while the MAD provides a measure of the average distance of shoreline positions from the mean.

In general, from 1990 to 2023, Transect 1 experienced significant erosion and accretion, with a general tendency toward erosion but a rapid accretion rate in the last three years. This transect exhibited high variability, as indicated by its relatively high standard deviation and MAD. Transect 2, over the same period, showed a general trend of accretion with lower variability, evidenced by its lower standard deviation and MAD compared to other transects, suggesting greater stability or less fluctuation in shoreline positions. However, in the last three years, transect 2 has shown a negative trend or erosion tendency. Transect 3 displayed a nearly stable shoreline position over the observed period, with a low mean indicating minimal net change. The standard deviation and MAD for this transect suggest moderate variability around this mean position, with an accretion trend observed in the last three years.

For the discussion, the observation period will be divided into two main segments. The first segment covers historical shoreline trends from 1990 to 2020, further divided into three distinctive periods: (i) 1990 – 2008, which can be generalized as having similar trends; (ii) 2009 – 2014; and (iii) 2015 – 2020, during which significant changes in shoreline position trends, particularly in Transect 1, were observed. The second segment focuses on recent shoreline detection from 2020 to

2023, detailing the most recent trends in shoreline position across the study area and discussing changes due to the construction of jetties and groins in 2021 at Pagatan Beach.

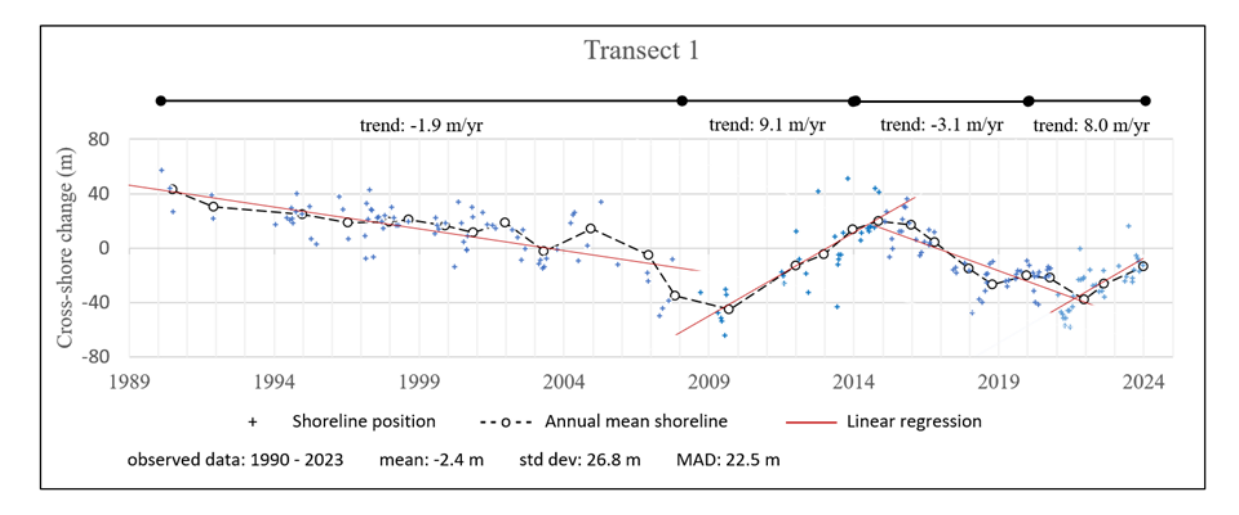


Figure 4. (a) Horizontal Position of Shoreline Changes in Transect 1 at Pagatan Beach

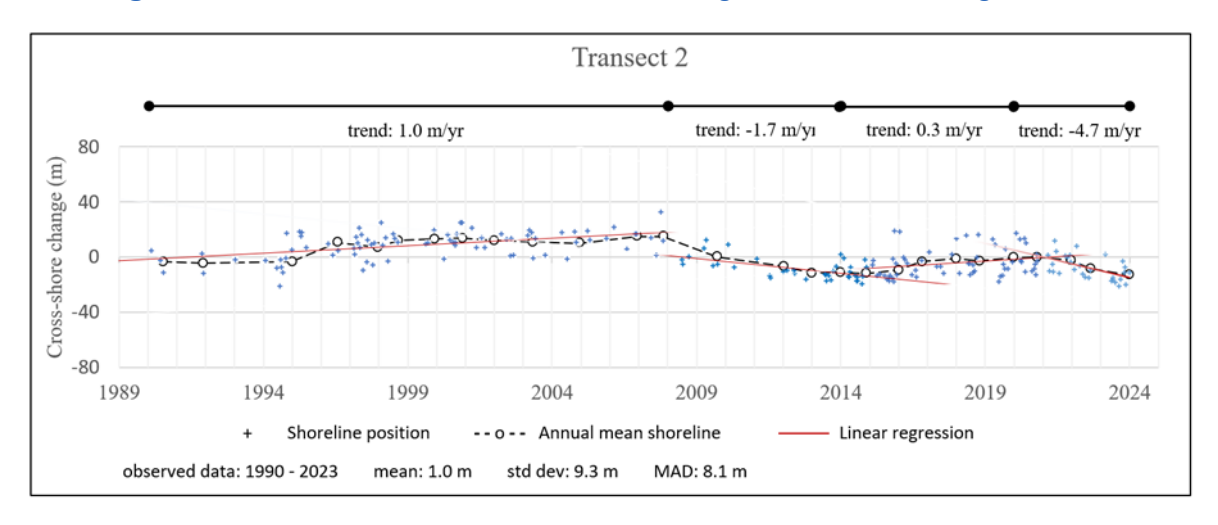


Figure 4. (b) Horizontal Position of Shoreline Changes in Transect 2 at Pagatan Beach

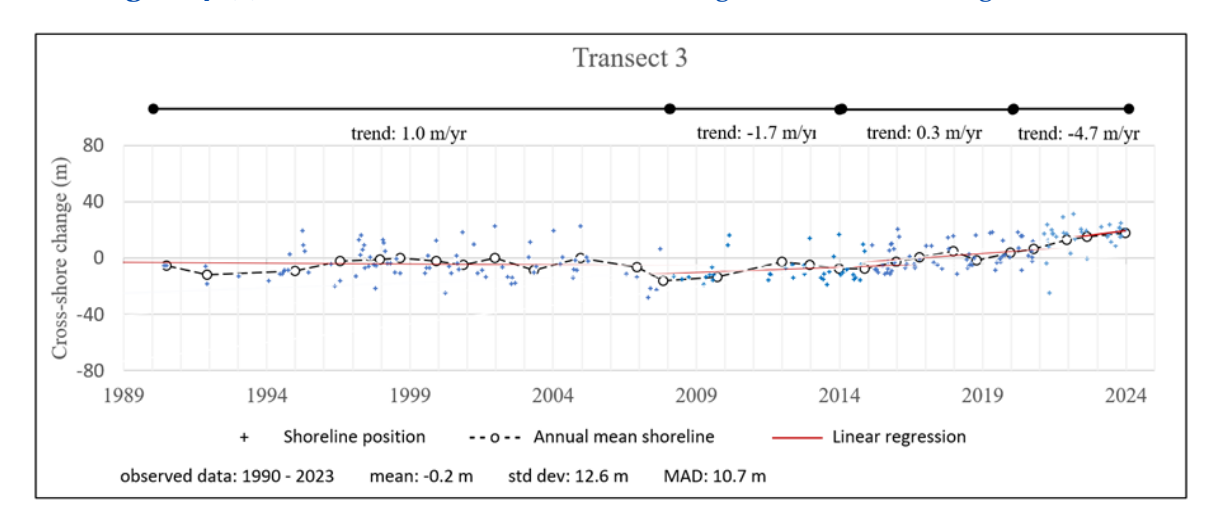


Figure 4. (c) Horizontal Position of Shoreline Changes in Transect 3 at Pagatan Beach

4. Discussion

4.1. Limitations and Challenges

The primary limitation of this study lies in achieving comprehensive spatial and temporal resolution, which affects the complete representation of beach variability. Satellite data before 2013 is sparse, affecting the accuracy of historical shoreline positions. The quality of satellite images (as illustrated in Figure 2) varies across different satellite missions with Landsat 5 (1990-2011), Landsat 7 (from 1999, with data gaps since 2003), and Landsat 8 (from 2013) provide images of increasing quality. This variation in image quality introduces potential biases, as more recent data may capture finer details and may provide more images, leading to inconsistencies when comparing historical and modern shoreline positions. However, the satellite imagery data can still be used to extract shoreline positions and provide insights into historical beach changes in the absence of in situ measurements in the study area. To cope with this limitation, only satellite images with a geo-accuracy of less than 10 meters were used for analysis, ensuring that the inaccuracy remains within the pixel size of the visible band, which is 30 meters.

Another challenge is the high cloud cover over the study area in Pagatan Beach, located near the equator, which reduces the number of usable images for shoreline extraction. To minimize inaccuracies due to cloud cover, only images with less than 10% cloud cover over the region of interest were utilized. Consequently, this criterion significantly reduced the number of available images for shoreline extraction that could represent the shoreline dynamics over the study period.

Furthermore, potential sources of error such as wave set-up, swash, and run-up dynamics have not been explicitly addressed in this analysis of shoreline changes at Pagatan Beach. The study did not incorporate topographic variations or beach slope, and tidal corrections were omitted due to the absence of local tide gauge data. Despite these limitations, CoastSat, a tool validated in micro-tidal environments, proved effective in accurately extracting shoreline positions with sub-pixel precision [8, 13, 15].

4.2. Shoreline Detection at Pagatan Beach

The shoreline dynamics at Pagatan Beach from 1990 to 2023 were seemed to be influenced by natural processes such as sea surface waves, sediment transport currents, tides, and wind, alongside significant human interventions like the construction of jetties and groins. The discussion will be divided into two main segments. The first segment examines historical shoreline trends from 1990 to 2020, detailing long-term changes. The second segment focuses on recent shoreline detection from 2020 to 2023, highlighting the latest trends influenced by the construction of jetties and groins in 2021 at Pagatan Beach. For this discussion, Table 3 summarizes the observed coastal changes across each transect as shown in Figure 4 in section 3 during the study period.

Table 3. Summary of Coastal Change Observed in Each Transects

| Observation period | Transect | Mean (m) | Standard deviation (m) | Mean absolute deviation (m) | Rate (meter /year) | Trend |
|--------------------|----------|-------------|------------------------------|-----------------------------------|--------------------------|-----------|
| 1990 – 2008 | 1 | 12.5 | 21.0 | 16.2 | -1.9 | Erosion |
| | 2 | 8.3 | 7.1 | 5.7 | 1.0 | Accretion |
| | 3 | -4.5 | 11.2 | 8.8 | -0.1 | Erosion |
| 2009 – 2014 | 1 | -1.2 | 34.5 | 27.7 | 9.1 | Accretion |
| | 2 | -8.1 | 5.0 | 3.8 | -1.7 | Erosion |
| | 3 | -7.2 | 9.8 | 7.4 | 0.3 | Accretion |
| 2015 – 2020 | 1 | -9.6 | 19.6 | 15.6 | -3.1 | Erosion |
| | 2 | -2.8 | 3.4 | 2.3 | 0.3 | Accretion |
| | 3 | 1.4 | 9.1 | 7.7 | 0.4 | Accretion |
| 2021 – 2023 | 1 | 27.3 | 17.0 | 13.5 | 12.4 | Accretion |
| | 2 | -7.7 | 5.4 | 3.8 | -4.7 | Erosion |
| | 3 | 15.4 | 10.2 | 6.6 | 2.6 | Accretion |

4.2.1. Historical Shoreline Trends (1990 – 2020)

The historical shoreline trends from 1990 to 2020 are analyzed in three distinct periods, focusing on significant changes in shoreline positions, particularly in Transect 1. These periods are delineated as 1990 - 2008, 2009 - 2014, and 2015 - 2020.

From 1990 to 2008, there were no significant or abrupt changes in shoreline positions across all transects. The shoreline changes observed during this period were likely driven by natural forces, including sea surface waves, sediment transport currents, tides, and wind. Studies along the South Kalimantan coast suggest that dominant wave energy originates from the south and southeast, influencing shoreline positions on sandy beaches in the region [16]. Transect 2 exhibited a consistent accretion rate of 1.0 m/year, while Transect 3 experienced steady erosion at a rate of 0.1 m/year, both showing low variability indicated by low standard deviation and mean absolute deviation (MAD) values. In contrast, Transect 1 showed significant erosion at a rate of -1.9 m/year, likely influenced by proximity to the river. Further studies considering tidal currents and sediment supply from the river are necessary for a comprehensive understanding of these historical changes.

Between 2009 and 2014, abrupt changes in shoreline trends were observed across all transects. Transect 2 shifted from accretion to erosion at a rate of -1.7 m/year, while Transect 3 transitioned from slight erosion to slight accretion at a rate of 0.3 m/year. Transect 1 experienced significant accretion at 9.1 m/year, possibly due to the suspected construction of a nearby jetty, inferred from satellite imagery revealing subtle structural features. Although no records confirm the exact timing of jetty construction and beach nourishment activities, the high accretion trend in Transect 1 suggests a plausible correlation with these construction activities.

Between 2014 and 2020, notable changes occurred in Transect 1, possibly due to the observed deterioration of a nearby jetty in satellite images from 2019. The jetty appeared to have suffered damage during this period. Transect 2 returned to experiencing accretion, likely influenced by sediment supply from Transect 1, where wave energy from the south and southeast directions affects longshore sediment movement towards Transects 2 and 3. In Transect 3, the sustained accretion rate may be attributed to jetty construction along the river in this section, which restricts sediment movement in the southeast direction.

4.2.2. Recent Shoreline Detection (2020 – 2023)

From 2020 to 2023, recent shoreline detection using satellite imagery revealed notable changes in the shoreline position trends within the study area. This period is marked by the reconstruction of the jetty and the construction of groins around Transect 1 in 2021, as observed in satellite images. These constructions significantly influenced shoreline changes during this period.

In Transect 1, accretion re-occurred at a rate of 8.0 m/year, with the groins effectively stabilizing the shoreline and maintaining sediment along approximately 500 meters of the shore. In Transect 2, erosion re-emerged at a rate of -4.7 m/year. This may be attributed to the influence of the groins, as natural forces from the south and southeast, or the sediment transport direction from Transect 1 to Transect 3, resulted in most sediment being trapped around Transect 1, leading to net erosion in Transect 2. Conversely, Transect 3 continued to experience accretion at an increased rate of 2.6 m/year, likely due to the jetty near Transect 3, which helped maintain sediment movement in the southeast direction.

The shoreline changes in Pagatan Beach from 1990 to 2023 were likely influenced by several factors, including natural forces such as sea surface waves, sediment transport currents, tides, and wind. Additionally, human interventions, such as the construction of jetties and groins over the observed period, significantly shaped the shoreline trends. Further research is still needed to comprehensively assess the historical records of these influences and understand their cumulative impact on the shoreline dynamics.

4.3. Map of Shoreline Change Risk

The trends derived from shoreline extraction data spanning the recent period from 2020 to 2023, following the construction of groins, were utilized to forecast future shoreline positions for 2025 and 2028. The erosion and accretion rates observed in 2023 served as the baseline for projecting shoreline dynamics. These trends were analyzed across three transects, and interpolations between transects were conducted to estimate changes throughout the study area. Figure 5 illustrates the map of risk based on these projections.

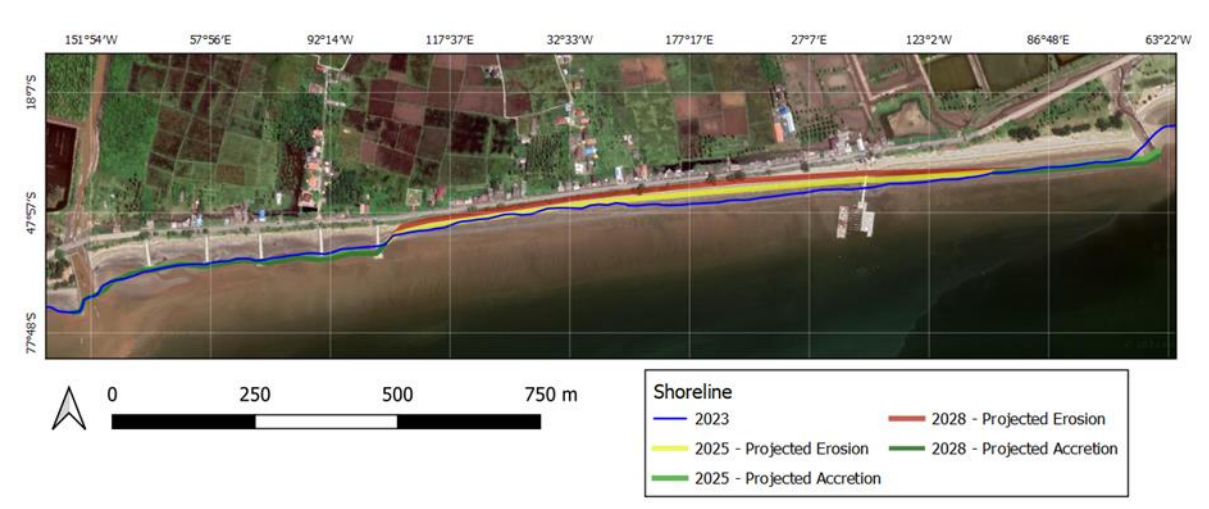


Figure 5. Map of Shoreline Change Risk in Pagatan Beach

According to the projections (see Figure 5), areas within approximately 500 meters west of the study area, where groins have been installed, are likely to continue experiencing accretion. The groins effectively maintain sediment within this zone up to their maximum length. Similarly, sections around the jetty located at the easternmost part of the study area show a consistent accretion trend, indicating effective sediment control by the jetty structure. This stability is anticipated to persist until 2028, assuming the groins and jetty continue to manage sediment effectively.

In contrast, a persistent erosion trend is anticipated along a 1-kilometer stretch in the central zone of the study area. By 2025, erosion is expected to continue, gradually reducing the beach area. Without intervention measures by 2028, there is a risk that erosion could encroach onto adjacent roads. Notably, a newly constructed offshore building in this section, observed in satellite imagery from 2021, is situated in an area prone to ongoing erosion. Further investigation is imperative to assess the structural stability of this building, focusing particularly on its foundation and the connecting bridge to the main road.

5. Conclusion

In conclusion, this study of Pagatan Beach's shoreline dynamics from 1990 to 2023 has underscored the complex interplay between natural processes and human interventions. Utilizing satellite imagery and CoastSat tools, we identified significant shifts in erosion and accretion trends, driven by factors such as waves, currents, tides, and wind, alongside the impacts of coastal structures like groins and jetties. The analysis revealed distinct patterns across different transects, with notable variability in shoreline changes. Notably, the construction of jetties and groins has played a crucial role in stabilizing certain areas, while also contributing to erosion in others, highlighting the need for careful management of coastal defenses.

Continued monitoring and adaptive management are essential for addressing the challenges posed by ongoing coastal changes. The projections indicate that without intervention, certain areas could face severe erosion risks, potentially affecting infrastructure and local communities by 2028. This study reinforces the importance of integrating coastal management practices with scientific monitoring to enhance resilience and mitigate the impacts of erosion and sediment dynamics. Future research should focus on refining these projections and exploring sustainable solutions to safeguard Pagatan Beach's coastal ecosystem and human assets.

6. Conclusion

Future research should incorporate in situ measurements of wave action, currents, tides, and wind to validate and refine satellite imagery analyses, enhancing the accuracy of shoreline change predictions. Detailed investigations into the impacts of coastal structures like groins and jetties on sediment transport and shoreline stability are essential. Utilizing higher-resolution satellite imagery and newer remote sensing technologies can improve detection and monitoring of subtle shoreline changes. Extending the study period and geographical scope will provide a broader understanding of regional coastal processes and trends, crucial for assessing the impacts of climate change, sea-level rise, and human activities on coastal areas.

7. Conclusion

This research adheres to ethical standards by using publicly accessible satellite imagery data from USGS, ensuring compliance with data use policies. Privacy and confidentiality of individuals and entities in coastal regions are respected. The study balances environmental impact and community well-being in its recommendations for coastal defenses, emphasizing the importance of stakeholder engagement in Pagatan Beach. Transparency in methodologies, findings, and limitations is maintained to uphold scientific integrity. The research highlights the need for ongoing monitoring and adaptive management to address evolving coastal dynamics ethically.

Author Contributions:

Conceptualization, A.A. Fitriadin and D.Y. Hardiani; methodology, A.A. Fitriadin; software, A.A. Fitriadin; validation, A.A. Fitriadin, D.Y. Hardiani and E.Anggraini; formal analysis, A.A. Fitriadin and E. Anggraini; investigation, A.A. Fitriadin and E. Anggraini; resources, A.A. Fitriadin, D.Y. Hardiani and E.Anggraini; data curation, A.A. Fitriadin; writing—original draft preparation, A.A. Fitriadin; writing—review and editing, D.Y. Hardiani and E.Anggraini; visualization, A.A. Fitriadin; supervision, D.Y. Hardiani.; project administration, E.A. Anggraini; funding acquisition, D.Y. Hardiani. All authors have read and agreed to the published version of the manuscript.

Conflicts of Interest:

The authors declare no conflicts of interest.

References

- R. Dolan, S. F. Michael, and J. H. Stuart, "Temporal Analysis of Shoreline Recession and Accretion," Journal of Coastal Research, vol. 7, no. 3, pp. 723-744, 1991. https://www.jstor.org/stable/4297888
- T. A. Łabuz, "Environmental Impacts—Coastal Erosion and Coastline Changes," in The BACC II Author Team (eds) Second Assessment of Climate Change for the Baltic Sea BasinRegional Climate Studies ed.: Springer, Cham, 2015. doi: https://doi.org/10.1007/978-3-319-16006-1_20 E. Boak and I. Turner, "Shoreline definition and detection: A review," J. Coast. Res., vol. 21, no. 4, pp. 688-703,
- 2005. doi: https://doi.org/10.2112/03-0071.1
- M. Shoshany and A. Degani, "Shoreline Detection by Digital Image Processing of Aerial Photography," Journal of Coastal Research, vol. 8, no. 1, pp. 29-34, 1992. https://www.jstor.org/stable/4297949
- C. J. Hapke, E. A. Himmelstoss, M. G. Kratzmann, J. H. List, and E. R. Thieler, "National assessment of shoreline change: Historical shoreline change along the New England and Mid-Atlantic coasts," US Geological Survey 2010. https://tamug-ir.tdl.org/bitstream/1969.3/29280/1/ofr2010-1118 report 508 rev042312.pdf
- N. Gorelick, M. Hancher, M. Dixon, S. Ilyushchenko, D. Thau, and R. J. R. s. o. E. Moore, "Google Earth Engine: everyone," Planetary-scale geospatial analysis for vol. https://doi.org/10.1016/j.rse.2017.06.031
- P. G. da Silva, M. S. Jara, R. Medina, A.-L. Beck, and M. A. J. C. E. Taji, "On the use of satellite information to detect coastal change: Demonstration case on the coast of Spain," vol. 191, p. 104517, 2024. doi: https://doi.org/10.1016/j.coastaleng.2024.104517
- S. Zollini et al., "New Methodology for Shoreline Extraction Using Optical and Radar (SAR) Satellite Imagery," vol. 11, no. 3, p. 627, 2023. doi: https://doi.org/10.3390/jmse11030627
- K. Vos, K. D. Splinter, M. D. Harley, J. A. Simmons, and I. L. Turner, "CoastSat: A Google Earth Engine-enabled Python toolkit to extract shorelines from publicly available satellite imagery," Environmental Modelling & Software, vol. 122, p. 104528, 2019/12/01/ 2019. doi: https://doi.org/10.1016/j.envsoft.2019.104528
- 10. A. Luijendijk, G. Hagenaars, R. Ranasinghe, F. Baart, G. Donchyts, and S. Aarninkhof, "The State of the World's Beaches," Scientific Reports, vol. 8, 2018. doi: https://doi.org/10.1038/s41598-018-24630-6
- 11. M. I. Vousdoukas et al., "Sandy coastlines under threat of erosion," vol. 10, no. 3, pp. 260-263, 2020. doi: https://doi.org/10.1038/s41558-020-0697-0
- 12. G. Hagenaars, S. de Vries, A. P. Luijendijk, W. P. de Boer, and A. J. H. M. Reniers, "On the accuracy of automated shoreline detection derived from satellite imagery: A case study of the sand motor mega-scale nourishment," Engineering, Coastal vol. pp. 113-125, 2018/03/01/ 2018. doi: https://doi.org/10.1016/j.coastaleng.2017.12.011
- 13. K. Vos, M. D. Harley, K. D. Splinter, J. A. Simmons, and I. L. Turner, "Sub-annual to multi-decadal shoreline variability from publicly available satellite imagery," Coastal Engineering, vol. 150, pp. 160-174, 2019/08/01/ 2019. doi: https://doi.org/10.1016/j.coastaleng.2019.04.004

- 14. B. Castelle et al., "Satellite-derived shoreline detection at a high-energy meso-macrotidal beach," Geomorphology, vol. 383, p. 107707, 2021/06/15/2021. doi: https://doi.org/10.1016/j.geomorph.2021.107707
- 15. C. Billet, G. Bacino, G. Alonso, and W. J. W. Dragani, "Shoreline Temporal Variability Inferred from Satellite Images at Mar del Plata, Argentina," vol. 15, no. 7, p. 1299, 2023. doi: https://doi.org/10.3390/w15071299
- 16. D. Darmiati, I. W. Nurjaya, and A. S. Atmadipoera, "Analysis of Shoreline Change in West Coast Area of Tanah Laut District South Kalimantan," Jurnal Ilmu dan Teknologi Kelautan Tropis, vol. 12, no. 1, pp. 211-222, 2020. doi: https://doi.org/10.29244/jitkt.v12i1.22815
- 17. I. Alifdini, R. A. Kismawardhani, A. Wirasatriya, D. N. Sugianto, O. b. Yaakob, and A. B. Widodo, "Identification of Tidal Energy Resources using Satellite Altimetry Data for Indonesian Seas," in 2018 4th International Symposium on Geoinformatics (ISyG), 2018, pp. 1-6. doi: https://doi.org/10.1109/isyg.2018.8611798
- 18. H. Xu, "Modification of normalised difference water index (NDWI) to enhance open water features in remotely sensed imagery," International Journal of Remote Sensing, vol. 27, no. 14, pp. 3025-3033, 2006. doi: https://doi.org/10.1080/01431160600589179